

# High poloidal beta long-pulse experiments in the Tokamak Fusion Test Reactor\*

J. Kesner†

Plasma Fusion Center, Massachusetts Institute of Technology, Cambridge, Massachusetts 02139

M. E. Mauel, G. A. Navratil, and S. A. Sabbagh

Columbia University, New York, New York 10027

M. Bell, R. Budny, C. Bush, E. Fredrickson, B. Grek, A. Janos, D. Johnson,

D. Mansfield, D. McCune, K. McGuire, H. Park, A. Ramsey,

E. Synakowski, G. Taylor, and M. Zarnstorff

Princeton Plasma Physics Laboratory, Princeton, New Jersey 08543

S. H. Batha and F. M. Levinton

Fusion Physics & Technology, Torrance, California 90503

(Received 8 December 1992; accepted 17 March 1993)

Experiments have been performed in the Tokamak Fusion Test Reactor [D. M. Meade *et al.* in *Plasma Physics Controlled Nuclear Fusion Research, 1990* (International Atomic Energy Agency, Vienna, 1991), Vol. 1, p. 9] with neutral beam injection of up to 4 sec. duration, which is comparable to the time scale for resistive redistribution of the plasma current profile. These plasmas were created using a rapid decrease of the plasma current which initially created a plasma with enhanced stability and confinement. As the current profile evolved, a significantly reduced beta limit was observed. The high  $\epsilon\beta_p$  plasmas had up to 90% of the current driven noninductively which significantly broadened the current profile during the long pulse lengths. These experiments demonstrated that high  $\beta_N$  plasmas could not be sustained for times longer than the resistive relaxation of the outer current region which at early times after the current ramp-down carried negative current. At later times in lower  $\beta_N$  discharges, beta collapses were sometimes observed as the current profile broadened at  $\beta_N \sim 1.5$ . The appearance of disruptions was consistent with the predictions of ideal magnetohydrodynamics (MHD) stability analyses.

## I. INTRODUCTION

Experiments performed in the Tokamak Fusion Test Reactor<sup>1</sup> (TFTR) have demonstrated the simultaneous achievement<sup>2-4</sup> of high poloidal beta ( $\beta_p \sim 6$ ,  $\epsilon\beta_p > 1.5$ ), high normalized beta ( $\beta_N \equiv aB_T\beta/I_p > 4.5$  mT%/MA), and high confinement ( $\tau_E/\tau_L > 3.5$ ) relative to the ITER-89P expression for L-mode confinement,  $\tau_L$ .<sup>5</sup> Here  $\beta_p$  is the poloidal beta (determined from diamagnetism),  $\beta_p \equiv 2\mu_0 \int V_p p dV / (V_p B_{pa}^2)$  with  $V_p$  the plasma volume,  $B_{pa} = \mu_0 I_p / \Gamma$  and  $\Gamma$  is the circumference of the plasma boundary. The normalized beta may be expressed as  $\beta_N = 20\epsilon\beta_p/q_*$  with  $q_* = (2\pi/\mu_0)(a^2 B_T / RI_p)(1 + \kappa^2)/2$  and  $\epsilon = a/R \approx 1/3$ . These discharges were produced with a rapid decrease in plasma current which transiently generated a high internal inductance current profile [with internal inductance defined as  $l_i = \int V_p B_p^2 dV / (V_p B_{pa}^2)$ ] having a reduced or reversed edge current. In these relatively short-pulse discharges the high normalized beta phase ( $\beta_N > 3$ ) was maintained no longer than 0.8 sec, which is much less than the current relaxation time. In high poloidal beta discharges the bootstrap current fraction was calculated to be large and the bootstrap current density peaks off axis, but broadening of the current profile was minimized by the short-pulse length. Other large tokamaks have conducted

high poloidal beta experiments with high bootstrap fractions. The Japan Tokamak-60 (JT-60) experiment<sup>6</sup> observed fast beta collapses. High poloidal beta experiments in the Joint European Tokamak (JET)<sup>7,8</sup> observed a regime of improved plasma confinement which ended in a beta collapse. Experiments on Doublet-III-D (DIII-D),<sup>9</sup> have documented the sensitivity of stability to profiles in relatively short pulsed experiments.<sup>10</sup>

In the present study, the neutral beam heating pulse in TFTR was extended to 4 sec to observe the current profile relaxation effects on plasma confinement and stability. It was found that discharges with high normalized beta,  $\beta_N > 3$  and similar to those reported from earlier experiments in TFTR,<sup>2-4</sup> could not be sustained for more than 0.8 sec of neutral beam heating. However, when lower power levels were used, discharges with  $\beta_N \lesssim 2$  could be sustained for the length of the heating pulse although beta collapses tended to occur near  $\beta_N \sim 1.5$ . The beta collapses were usually associated with 3/2 and 2/1 modes similar to observations made on other devices.<sup>11</sup> Although stability limits were profoundly reduced during the current evolution, the enhanced energy confinement ( $\tau_E/\tau_L > 3$ ) achieved after the current ramp was maintained throughout the discharge whenever there was no magnetohydrodynamic (MHD) activity.

In order to understand the decrease in stability as the current evolved, simulations of the experimental discharges were performed using the interpretive transport

\*Paper 413, Bull. Am. Phys. Soc. 37, 1439 (1992).

†Invited speaker.

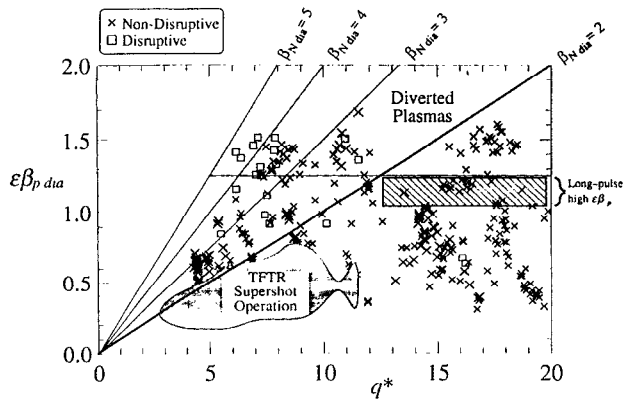


FIG. 1. High  $\epsilon\beta_p$  database displayed in  $\epsilon\beta_p$  vs  $q_*$  space. The cross-hatched area shows the operating space for long-pulse experiments.

code, TRANSP.<sup>12</sup> The current profile calculated with TRANSP could be compared with motional Stark effect (MSE) measurements<sup>13</sup> of the local magnetic field pitch angle and combined with calculated pressure profiles to determine the ideal MHD stability as the profile evolved. The simulations identified two time scales associated with the current profile evolution: (1) the resistive diffusion time scale of the core plasma current density and (2) the resistive time scale of the outer plasma. Measurements of the evolution of the on-axis safety factor,  $q_0[q_0 \equiv q(r=0)]$ , characterize the evolution of the current density in the plasma core while the internal inductance,  $l_i$ , characterizes the edge-weighted moment of the current profile.

The observations and calculations reported here illustrate the tendency of high  $\epsilon\beta_p$  discharges to develop reduced beta limits as noninductive, steady-state conditions are approached. The experiments furthermore demonstrate the need for edge current profile control if the high  $l_i$ , high  $\beta_N$  current profiles produced after the current ramp-down are to be maintained in steady-state discharges with high bootstrap fractions.

Figure 1 shows the  $\epsilon\beta_p$  vs  $q_*$  operating space that is accessible in TFTR, and it provides a useful way to introduce the relationship between the long-pulse experiments reported here and earlier high  $\epsilon\beta_p$  experiments. In this diagram, Troyon's stability limit<sup>14</sup> ( $\beta_N \leq C_T$ , with  $C_T$  a constant for fixed current profiles) is given by a straight line through the origin. In previous experiments, discharges would reach  $\beta_N \approx 3$  for relatively short durations of beam heating and, if they reached much higher  $\beta_N$  or lasted longer, they tended to suffer beta collapses or disruptions. In the present long-pulse experiments, we maintained discharges for the full 4 sec duration of the neutral beam heating pulse while at the same time achieving conditions producing a large bootstrap current fraction. However, since  $\beta_N > 3$  could not be sustained for long pulses, we were required to operate within a restricted region of  $q_*$  having lower  $\beta_N$ . This region is shown with cross-hatched in Fig. 1. Within this region  $\beta_p$  was high in order to obtain a high bootstrap current fraction, approximately given by  $f_B \equiv (I_{BS}/I_p) \propto \beta_p / \sqrt{\epsilon}$ .<sup>15</sup> The values of the plasma current

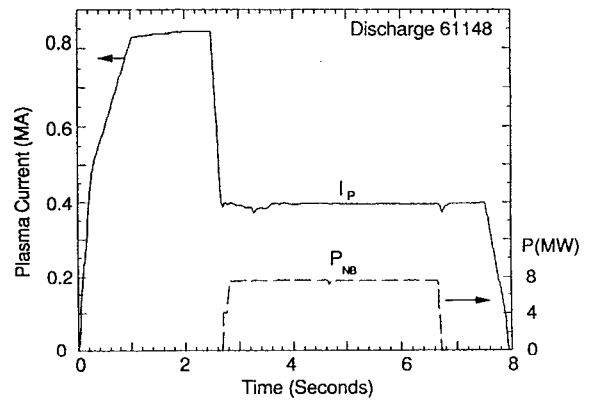


FIG. 2. Plasma current (MA) and neutral beam power (MW) for discharge 61148.

were determined by the intersections of the stability limit (characterized by the attainable Troyon value,  $C_T$ ) and the equilibrium poloidal beta limit<sup>3</sup> (approximately  $\epsilon\beta_p < 1.5$ ). For the profiles studied by Troyon,<sup>14</sup>  $C_T \sim 3$  allowing  $q_* = 20\epsilon\beta_p/C_T \sim 8$  for  $\epsilon\beta_p \sim 1$ . However, since  $C_T$  degrades as the current profile broadens,  $C_T \sim 2$  implies  $q_* \sim 15$  as indicated in Fig. 1. A final operational consideration for the long-pulse experiments was the need to maintain sufficiently low plasma density so that  $\nu_* \lesssim 0.1$  (where  $\nu_*$  is ratio of the effective collision frequency to the bounce frequency  $\nu_* \propto n_e$ ), as is required for high values of  $f_B$ . For these experiments, the wall conditioning was very good, and the line-averaged electron density was maintained below  $3 \times 10^{13} \text{ cm}^{-3}$  while  $T_e(0)$  ranged between 5 and 7 keV.

The remainder of this paper is organized into four sections. Section II describes the experimental conditions required to achieve 4 sec discharges having high  $\epsilon\beta_p$ . Section III presents calculations of the ideal  $n=1$  and  $n=\infty$  MHD stability during several times during the discharge evolution. In addition, the approximate beta limit for plasmas within the first stability regime described by Wesson and Sykes<sup>16</sup> is used to show a relatively straightforward relationship between the  $q$  profile and stability. Section IV describes observations of the nearly constant energy confinement as the current profile evolves, and Sec. V contains conclusions.

## II. EXPERIMENTAL CONDITIONS

To obtain regimes of high  $\epsilon\beta_p$  and  $\beta_N$  in TFTR, the discharge was initiated with a relatively high plasma current which is subsequently ramped-down prior to neutral beam heating.<sup>2-4</sup> Figure 2 shows the plasma current and neutral beam power for a typical long-pulse discharge (shot 61148). In discharge 61148 the plasma current is ramped from 850 to 400 kA between  $t=2.5$  and  $2.7$  sec just prior to application of 8 MW of neutral beam power. The discharge is sawtooth free and the neutral beams drive a net positive current. Figure 3(a) shows the current density just before the  $I_p$  ramp-down ( $t=2.4$  sec), immediately after the ramp-down ( $t=2.8$  sec), and 2.5 sec after the

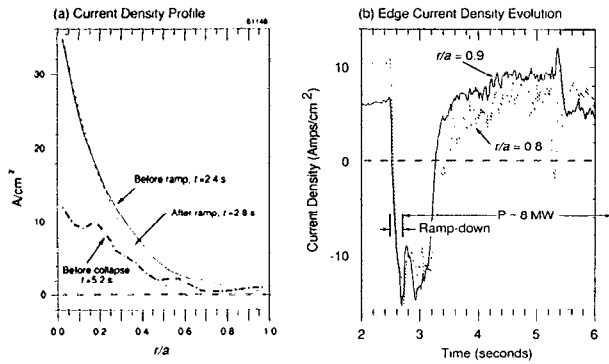


FIG. 3. TRANSP calculated current profile evolution for discharge 61148: (a) Current density versus normalized radius just before the current ramp-down at  $t=2.5$  sec, just after the ramp-down at  $t=2.7$  sec, and at  $t=5.2$  sec. (b) Current density ( $A/cm^2$ ) at  $r/a=0.8, 0.9$  versus time.

current ramp-down ( $t=5.2$  sec). The broadening of the current profile and drop in the central current density is evident. Figure 3(b) indicates the time evolution of current density near the plasma edge ( $r/a=0.8$  and  $0.9$ ). A negative skin current that carries a current fraction of  $I_{neg}/I_p=22\%$  at the maximum is calculated, and some current reversal persists for as long as  $0.7$  sec following the current ramp-down. The edge current density rises in time, and, after  $t=3.6$  sec, TRANSP indicates the development of a small bootstrap-driven current pedestal. Notice that the gradient of the current density reverses due to the bootstrap effect. Figure 4 displays the toroidal plasma voltage obtained from TRANSP just after current ramp-down and  $2.4$  sec after the ramp-down for the same discharge. At this time the loop voltage is nearly constant and close to zero throughout the radius (except near the magnetic axis) indicating that the discharge is close to resistive equilibrium.

Figure 5 displays  $\beta_p$  and beam heating interval, line density and  $H_\alpha$ , and Mirnov loop amplitudes (within the frequency bands  $5 < f < 15$  and  $25 < f < 35$  kHz) for discharge 61148. Here  $\epsilon\beta_p > 1$  until the beta collapse at  $t=5.2$  sec. This discharge was observed to sequentially pass

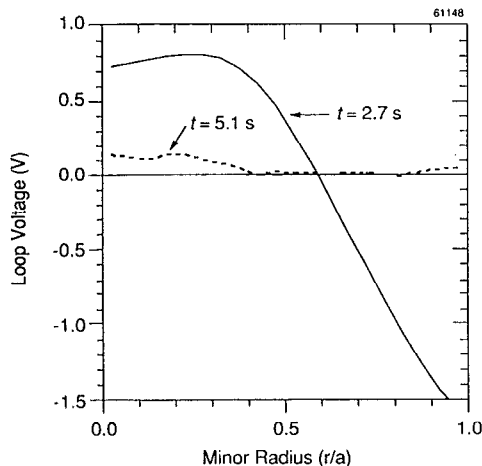


FIG. 4. Toroidal plasma voltage versus normalized radius just after and  $2.4$  sec after the ramp-down for discharge 61148.

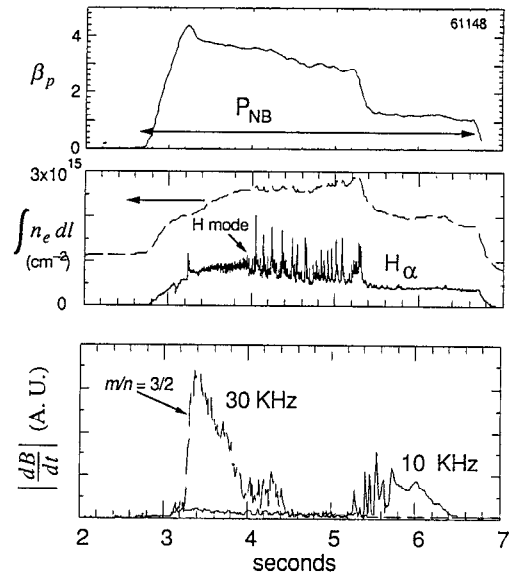


FIG. 5. (a)  $\beta_p$ , (b) electron line density and  $H_\alpha$ , (c) rectified amplitude of Mirnov loop signals (with the frequency bands  $5 < f < 15$  kHz and  $25 < f < 35$  kHz) for discharge 61148.

through the following states: (a) The Ohmic phase lasts until the current ramp-down at  $t=2.7$  sec. (b) The discharge is heated to the equilibrium limit characterized by the formation of a separatrix at  $t=2.9$  sec. (c) The  $3/2$  mode becomes unstable at  $t=3.2$  sec and a small beta collapse occurs. With the beta drop, the discharge becomes limited on the inside limiter. (d) A transition to a limiter H mode<sup>17</sup> takes place at  $t=3.9$  sec, followed by the onset of edge localized modes (ELM's) at  $t=4$  sec. (e) The  $3/2$  mode is stabilized at  $t=4.4$  sec as  $q_0$  rises. (f) A substitution of beam sources occurs at  $t=4.6$  sec and causes a density rise and an increase in ELM frequency. (g) A strong beta collapse occurs at  $t=5.2$  sec and plasma confinement becomes L mode.

Sufficiently elevated values of  $q_0$  should eliminate the  $m/n=2/1$  mode (when  $q_0 \gtrsim 2$ ) and the  $3/2$  mode (when  $q_0 \gtrsim 1.5$ ) that often hinder the attainment of high  $\beta_N$ . Indeed, this effect may have contributed to the stabilization of the  $3/2$  mode described above. Since the noninductive currents in these experiments significantly broadened the current profile,  $q_0$  rose throughout the pulse. Figure 6 compares  $q_0$  for discharge 61148 measured by the MSE diagnostic with the time evolution predicted by TRANSP. The calculated internal plasma inductance,  $l_i$ , is also shown. The particular beam source used for the MSE measurement was on for only 2 sec in this discharge. The MSE measurement follows the prediction closely up to  $q_0=1.4$  at  $t=4.6$  sec. The internal plasma inductance calculated by TRANSP decays from  $l_i > 4$  after the current ramp-down to 1 at  $t \sim 5$  sec (which is below the preramp Ohmic value of  $l_i$ ).

### III. MHD STABILITY

The extensive diagnostic capability of TFTR permits a direct determination of MHD stability boundaries. In

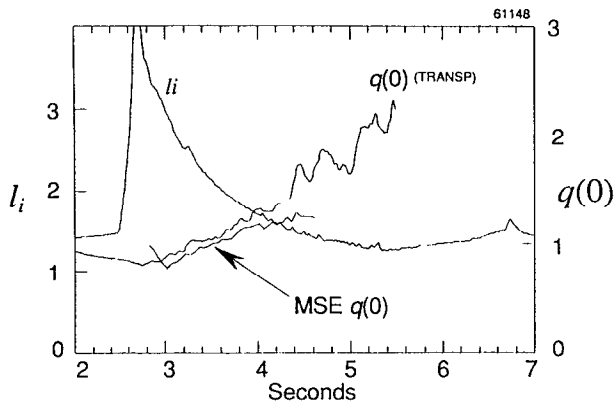


FIG. 6.  $q_0$  measured by MSE and predicted by TRANSP versus time in discharge 61148.  $I_i$  is also shown.

TFTR the electron temperature is determined from both a scanning electron cyclotron emission (ECE) system with independent calibration, and a Thomson scattering measurement. The electron density is determined from microwave interferometry, the ion temperature and plasma toroidal rotation from charge-exchange recombination spectroscopy (CHERS), and  $Z_{\text{eff}}$  from visible bremsstrahlung;  $q_0$  is determined by the MSE measurements. The TRANSP code calculates the neutral-beam-driven hot-ion density, pressure, and beam-driven current. TRANSP does not diffuse the suprathermal ions and this appears to be an appropriate approximation in the absence of MHD activity (such as 2/1 modes). TRANSP also calculates the bootstrap current and determines the current and  $q$ -profile evolution based on neoclassical resistivity.<sup>18</sup>

Disruptions and beta collapses in high  $\beta_N$  plasmas reduce confinement times and prevent the maintenance of the high beta plasma state. Figure 7 plots a database of high poloidal beta discharges that suffered disruptions or

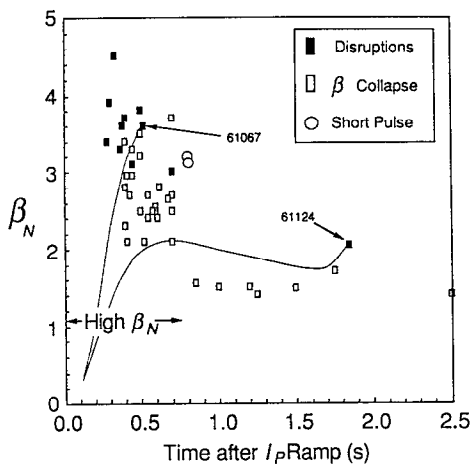


FIG. 7. A database of normalized beta at the onset of disruptions and beta collapses versus time after the current ramp-down. Also shown are the  $\beta_N$  values at the end of some "short-pulse" discharges (from in Ref. 1) which end at the end of the neutral beam heating pulse without a major MHD event. The time evolution of two disruptive discharges are superimposed.

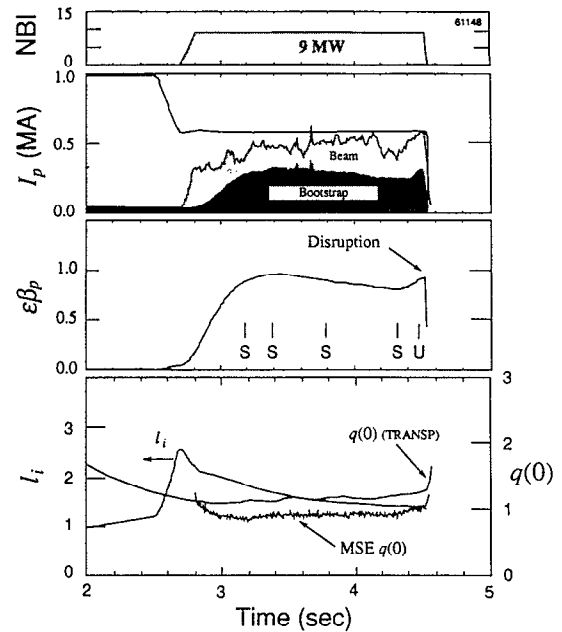


FIG. 8. Traces of beam power, plasma current,  $\epsilon\beta_p$ ,  $q(0)$ , and  $I_i$  for discharge 61124.

beta collapses as well as some "short-pulse" discharges which ended when neutral beam injection was switched off and before a major MHD event. The solid squares represent disruptions, the open squares represent beta collapses, and the circles represent "short-pulse" discharges. As more beam power was applied, disruptions were observed to occur earlier in time and at higher  $\beta_N$ . Some of the scatter in the data results from different current ramp ratios in the data set. A region of access to  $\beta_N > 3$  exists for  $\lesssim 0.8$  sec after the current ramp-down. This time is characteristic of the relaxation of the current profile in the outer portion of the plasma. In lower beta discharges ( $\beta_N \lesssim 2$ ) at later times beta collapses driven by 3/2 and 2/1 modes occurred at  $\beta_N \sim 1.5$  as the current profile broadened. The beta collapses often occurred as beta was dropping, indicating that these modes are sensitive to the evolving current profile. Beta collapses associated with 2/1 mode beta collapses are more virulent than 3/2 mode collapses and can result in the loss of half of the stored energy. Disruptions occur at higher  $\beta_N$  values than the beta collapses and usually occur as  $\beta_N$  is rising or at a maximum.

We will first examine discharge 61124 which ended in a disruption. In this discharge the current is ramped down from 1 to 0.6 MA prior to injection of 9 MW of predominantly co-injected neutral beams (Fig. 8). The beam and bootstrap-driven currents make up  $\sim 90\%$  of the total plasma current. Neutral beam heating begins at the end of the current ramp at  $t=2.7$  sec. The TRANSP simulation indicates that a negative current mantle exists for  $r/a \gtrsim 0.8$ , and the negative current disappears at  $t=3.2$  sec for  $r/a \sim 0.9$  and at 3.5 sec for  $r/a \sim 0.8$ . A small bootstrap pedestal with a reversal of the current gradient develops after  $t=3.5$  sec [similar to that shown in Fig. 3(b)]. At  $t=4.5$  sec beta rises and the discharge disrupts at a rela-

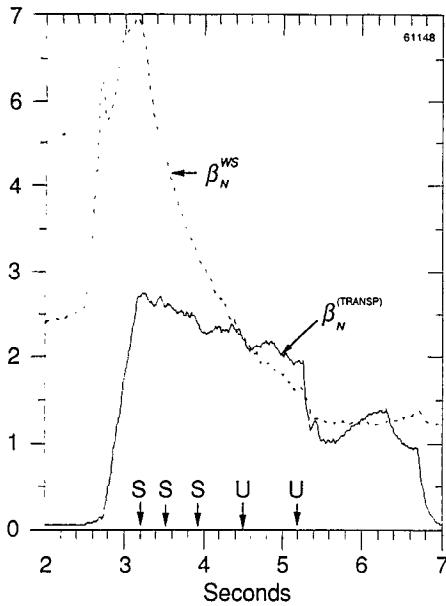


FIG. 9.  $\beta_N^{\text{TRANSP}}$  and  $\beta_N^{\text{WS}}$  for discharge 61148. In this figure,  $\beta_N^{\text{TRANSP}}$  is proportional to the total pressure calculated from TRANSP, and this differs slightly from the diamagnetic value due to an anisotropic pressure created by NBI.

tively low beta,  $\beta_N=2.3$ . Analyses of the stability of the plasma to ideal  $n=1$  free boundary modes were performed at several times using the PEST stability code<sup>19</sup> as indicated in the  $\epsilon\beta_p$  panel in Fig. 8. Here “S” indicates stability and “U” instability. These calculations predict the destabilization of an  $n=1$  pressure-driven kink/ballooning mode at the time of the disruption. The analysis shows that the maximum  $\beta_N$  at which the free-boundary  $n=1$  kink/ballooning mode is stable decreases continuously as the current profile relaxes and broadens up to the time of disruption. An  $n=\infty$  ballooning analysis was also performed, and it indicates that the outer half of the plasma is close to marginal stability at the end of the discharge.

In a similar but higher power ( $P_{NB}=12$  MW) discharge (61067) earlier in the same run, a disruption occurred at  $t=3.25$  sec and at  $\beta_N=3.6$ . This shot was representative of attempts to prolong discharges with  $\beta_N>3$ . Discharge 61067 had similar current and gas programming to 61124, but 15 MW of neutral beam heating power was applied to 61067 as compared with only 9 MW in 61124. Figure 7 also compares the  $\beta_N$  evolution for 61067 with 61124. Although the higher power shot succeeded in reaching high  $\beta_N$ , stability could not be maintained longer than the characteristic time scale of the current relaxation in the outer portion of the plasma.

Consider next the stability of discharge 61148 described in detail in the previous section. The beam and bootstrap currents were comparable and accounted for  $>70\%$  of the plasma current. The rise in  $q_0$  was shown in Fig. 6. This discharge suffered a strong beta collapse after 2.5 sec of beam heating, at a time when the current profile was close to equilibrium. Stability analysis for  $n=1$  ideal MHD free-boundary modes was performed at five times (Fig. 9) and instability was predicted at  $t=4.5$  sec (the

beta collapse occurred at  $t=5.2$  sec) as indicated in Fig. 9. We believe the small difference in time between the calculated onset of  $n=1$  instability and the observed beta collapse may be attributable to the uncertainty in the  $q$  profile predicted by TRANSP. An  $n=\infty$  ballooning analysis was also performed, and it indicates that the outer half of the plasma is marginally stable at  $t=5.2$  sec, when the beta collapse occurs. Experimentally the beta collapse appears as a 5 kHz mode which remains unstable from  $t=5.2$  sec until the end of the discharge.

Although numerical calculations can accurately determine the ideal MHD stability threshold, useful insight can also be obtained computing the approximate stability limit described by Wesson and Sykes.<sup>16</sup> This is especially appropriate for high  $q_*$  plasmas at marginal stability since  $n=1$  modes have been shown to have a ballooning character at all radii.<sup>20</sup> Alternatively, the critical mode number,<sup>21</sup>  $n_c$ , for high  $n$  ballooning drops toward 1 in high  $q_*$  plasmas. The  $n=\infty$  ballooning modes are driven by the pressure gradient  $p'$  and stabilized by shear. The ratio of drive to stabilization will determine an approximate stability condition,<sup>22</sup>  $\alpha/S \approx 0.6$ , with the shear parameter  $S=rq'/rq$  and the normalized pressure gradient  $\alpha=-2\mu_0 Rq^2 p'/B_T^2$ . By setting  $\alpha/S=0.6$  on all flux surfaces (marginal ballooning stability on all flux surfaces) Wesson and Sykes<sup>16</sup> obtained a critical beta

$$\beta_{\text{WS}} \equiv \frac{0.6\epsilon}{a^3} \int_0^a \frac{r^3 q'(r)}{q^3} dr,$$

where  $\beta_{\text{WS}}$  depends only on the  $q$  profile and provides a simple upper limit for  $\beta$ ;  $\beta_{\text{WS}}$  can be evaluated using TRANSP.

In shaped plasmas such as DIII-D,  $l_i$  is a directly measurable quantity and it has been shown that  $\beta_{\text{WS}} \sim (\epsilon/q_*^2)(l_i-0.5)$ .<sup>23</sup> For a cubic  $q$  profile  $\beta_{\text{WS}} \approx 0.3\epsilon/q_0 q_*$  which indicates an inverse dependence on the ballooning stability boundary with  $q_0$ . For TFTR plasmas,  $l_i$  is not directly measured, and we choose to calculate  $\beta_{\text{WS}}$  directly from the TRANSP-generated  $q$  profiles instead of using either approximation relating  $\beta_{\text{WS}}$  to  $l_i$  or to  $q_0$ .

The Wesson–Sykes critical beta for discharge 61148 is shown in Fig. 9. During this discharge  $\beta_N^{\text{WS}}$  varies from 6 to  $\approx 1.2$  indicating that a wide variation of the ballooning limit can occur in a single discharge as the current profile broadens. The experimental  $\beta_N$  exceeds the value of  $\beta_N^{\text{WS}}$  shortly before the observed beta collapse, and this may be attributed to the uncertainty of the calculated  $q$  profile.

Although the discharges immediately preceding and after 61148 were set up in an identical manner, they exhibited different MHD characteristics. Figure 10 displays the diamagnetism (mWb) (a measure of the transverse energy) and the 10 and 30 kHz fluctuation signals for discharges 61147 and 61148. In discharge 61147 a strong 2/1 beta collapse is observed at  $t=3.2$  sec, the time when 61148 had a weak 3/2 collapse. It would appear that the stability boundaries for the 3/2 and 2/1 mode are close to one another and the relaxation of the current profile caused by the 3/2 mode can prevent the destabilization of the 2/1

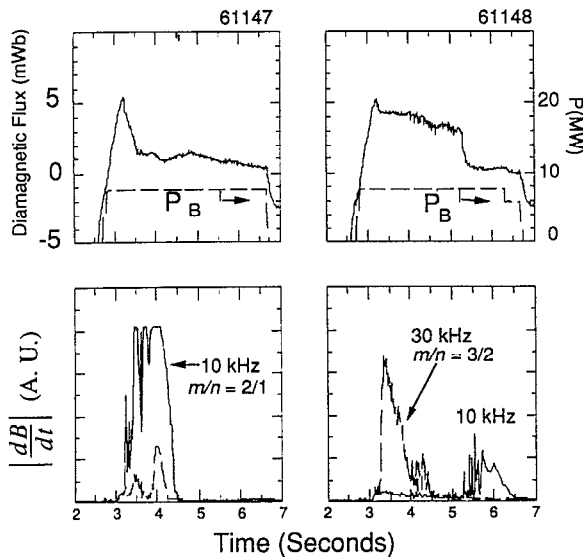


FIG. 10. Displaced toroidal flux (mWb), neutral beam power (arbitrary units) and  $f \sim 10$  and  $f \sim 30$  kHz Mirnov fluctuation signal for sequential discharges 61147 and 61148.

mode. The 2/1 mode present in discharge 61147 appears to stabilize after  $t = 4.6$  sec and  $\beta_N$  rises slightly.

#### IV. ENERGY CONFINEMENT

In these experiments the thermal component accounted for only 20%–50% of the total stored energy. Figure 11 indicates the energy confinement for total and thermal energy and  $l_i$  for discharge 61148. The energy confinement times are defined to be  $\tau_E \equiv \langle E_{\text{tot}} \rangle / P_{\text{inj}}$ ,  $\tau_E^{\text{th}} \equiv \langle E_{\text{thermal}} \rangle / P_{\text{inj}}$ .

As  $l_i$  drops from 2 to 1.2,  $\tau_E$  and  $\tau_E^{\text{th}}$  remain approximately constant. Thus energy confinement does not appear to degrade significantly as the current profile broadens. This contrasts with previous results that indicate that a

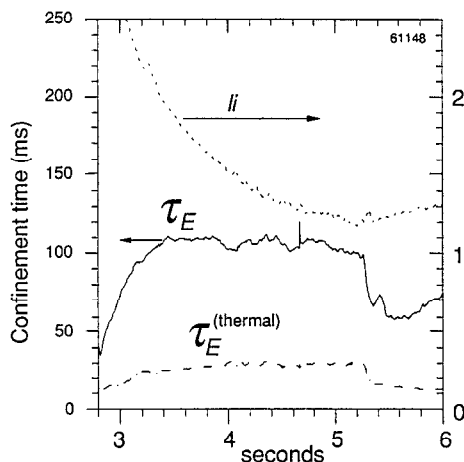


FIG. 11. Energy confinement for total and thermal energy and  $l_i$  for discharge 61148.

degradation of energy confinement accompanies the relaxation in  $l_i$  for L-mode discharges in TFTR<sup>24</sup> and for both L- and H-mode discharges in DIII-D.<sup>25</sup>

#### V. CONCLUSIONS

The plasma current ramp-down technique was used to produce plasmas with greater than 90% noninductive current fractions. The discharges have been maintained for a constant-current electric field relaxation time.<sup>26</sup> The current profile immediately after the ramp-down contained a negative current in the outer region which contained 15%–25% of the total plasma current. The current profile in the outer region typically relaxed on a time scale on the order of 0.7 sec while the current profile in the core of the plasma took several seconds to equilibrate.

High normalized beta ( $\beta_N > 3$ ) could not be sustained for longer than 0.8 sec, which is approximately the period for the relaxation of the outer portion of the plasma current. The accessibility of the high normalized beta regime in  $\epsilon\beta_p \sim 1$  discharges appears to be a result of the current profile created by the current ramp and characterized by a negative edge current, increased shear, and high  $l_i$ . Lower  $\beta_N$  discharges could be sustained for the full duration of the heating pulse although, as the current density profile broadens within the plasma core, beta collapses were often observed to occur near  $\beta_N \sim 1.5$ .

Energy confinement did not degrade as the current profile relaxed in these discharges. The  $I_p$  ramp-down plasmas access a confinement regime in which the plasma current profile does not appear to affect confinement for either the thermal or suprathreshold species.

These observations imply that maintenance of high normalized beta values can be obtained in high poloidal beta plasmas if current profile control is applied to maintain ramp-down-like current profiles. The broad current profiles that are present with high bootstrap fractions are subject to beta collapses at reduced values of  $\beta_N$ .

#### ACKNOWLEDGMENTS

We would like to thank M. Phillips and J. Manickam for providing the MHD equilibrium and stability codes. J. Kesner would like to thank J. Ramos, S. Luckhardt, and L. Zakharov for insightful discussions relating to MHD stability theory.

This work was performed under contract to the U.S. Department of Energy, Contracts No. DE-FG02-89ER53297 and No. DE-AC02-76-CHO-3073.

<sup>1</sup>D. M. Meade, V. Arunasalam, C. W. Barnes, M. G. Bell, R. Bell, M. Bitter, R. Boivin, N. L. Bretz, R. Budny, C. E. Bush, A. Cavallo, C. Z. Cheng, T. K. Chu, S. A. Cohen, S. Cowley, S. L. Davis, D. L. Dimock, J. Dooling, H. F. Dylla, P. C. Efthimion, A. B. Ehrhardt, R. J. Fonck, E. D. Fredrickson, H. P. Furth, R. J. Goldston, G. J. Green, B. Grek, L. R. Grisham, G. W. Hammett, R. J. Hawryluk, K. W. Hill, J. C. Hosea, R. B. Howell, H. Hsuan, R. A. Hulse, A. C. Janos, D. L. Jassby, F. C. Jobes, D. W. Johnson, L. C. Johnson, R. Kaita, S. M. Kaye, J. Kesner, C. Kieras-Phillips, S. J. Kilpatrick, H. Kugel, P. H. LaMarche, B. LeBlanc, D. M. Manos, D. K. Mansfield, E. S. Marmor, M. E. Mauel, E. Mazzucato, M. P. McCarthy, D. C. McCune, K. M. McGuire, S. S. Medley, D. R. Mikkelsen, D. A. Monticello, R. W. Motley, D. Mueller, J. Murphy, Y. Nagayama, G. A. Navratil, R. Na-

- zikian, D. K. Owens, H. K. Park, W. Park, S. F. Paul, R. Perkins, S. Pitcher, A. T. Ramsey, M. H. Redi, G. Rewoldt, D. R. Roberts, A. L. Roquemore, P. H. Rutherford, S. A. Sabbagh, G. Schilling, J. Schivell, G. L. Schmidt, S. D. Scott, J. Snipes, J. E. Stevens, W. Stodiek, B. C. Stratton, E. J. Synakowski, W. M. Tang, G. Taylor, J. L. Terry, J. R. Timberlake, H. H. Towner, M. Ulrickson, S. von Goeler, R. M. Wieland, M. Williams, J. R. Wilson, K. L. Wong, M. Yamada, S. Yoshikawa, K. M. Young, M. C. Zarnstorff, and S. J. Zweben, in *Plasma Physics Controlled Nuclear Fusion Research, 1990* (International Atomic Energy Agency, Vienna, 1991), Vol. 1, p. 9.
- <sup>2</sup>S. A. Sabbagh, R. A. Gross, M. E. Mauel, G. A. Navratil, M. G. Bell, R. Bell, M. Bitter, N. L. Bretz, R. V. Budny, C. E. Bush, M. S. Chance, P. C. Efthimion, E. D. Fredrickson, R. Hatcher, R. J. Hawryluk, S. P. Hirshman, A. C. Janos, S. C. Jardin, D. L. Jassby, J. Manickam, D. C. McCune, K. M. McGuire, S. S. Medley, D. Mueller, Y. Nagayama, D. K. Owens, M. Okabayashi, H. K. Park, A. T. Ramsey, B. C. Stratton, E. J. Synakowski, G. Taylor, R. M. Wieland, M. C. Zarnstorff, J. Kesner, E. S. Marmor, and J. L. Terry, *Phys. Fluids B* **3**, 2277 (1991).
- <sup>3</sup>M. E. Mauel, G. A. Navratil, R. J. Hawryluk, A. C. Janos, D. W. Johnson, D. C. McCune, K. M. McGuire, S. S. Medley, D. Mueller, D. K. Owens, H. K. Park, A. T. Ramsey, B. C. Stratton, E. J. Synakowski, G. Taylor, R. M. Wieland, M. C. Zarnstorff, J. Kesner, E. S. Marmor, and J. L. Terry, *Nucl. Fusion* **32**, 1468 (1992).
- <sup>4</sup>G. A. Navratil, R. A. Gross, M. E. Mauel, S. A. Sabbagh, M. G. Bell, R. Bell, N. L. Bretz, R. Budny, M. S. Chance, E. D. Fredrickson, R. Hatcher, R. J. Hawryluk, A. C. Janos, D. L. Jassby, D. C. McCune, K. M. McGuire, S. S. Medley, D. Mueller, M. Okabayashi, D. K. Owens, H. K. Park, B. C. Stratton, E. J. Synakowski, G. Taylor, R. M. Wieland, M. C. Zarnstorff, J. Kesner, E. S. Marmor, J. L. Terry, P. A. Politzer, L. L. Lao, G. D. Porter, C. D. Challis, M. S. Chu, A. D. Turnbull, E. J. Strait, D. Wroblewski, K. Matsuda, and the DIII-D Team, in Ref. 1, p. 209.
- <sup>5</sup>P. N. Yushmanov, T. Takizuka, K. S. Riedel, O. J. W. F. Kardaun, J. G. Cordey, S. M. Kaye, and D. E. Post, *Nucl. Fusion* **30**, 1999 (1990).
- <sup>6</sup>S. Ishida, Y. Koide, T. Ozeki, M. Kikuchi, S. Tsuji, H. Shirai, O. Naito, and M. Azumi, *Phys. Rev. Lett.* **68**, 1531 (1992).
- <sup>7</sup>C. D. Challis, T. C. Hender, J. O'Rourke, S. Ali-Arshad, B. Alper, H. J. deBlank, C. G. Gimblett, J. Han, J. Jacquinet, G. J. Kramer, W. Kerner, D. P. O'Brien, P. Smeulders, M. Stamp, D. Stork, P. M. Stuberfield, D. Summers, F. Tibone, B. Tubbing, and W. Swingmann, "High bootstrap ICRF plasmas in JET," submitted to *Nucl. Fusion* (1992).
- <sup>8</sup>The JET Team, presented by D. Stork, "Pulse operation of JET and its implications for a reactor," *Proceedings of the 14th International Conference Plasma Physics and Controlled Nuclear Fusion Research, 1992* (International Atomic Energy Agency, Vienna, in press), Paper IAEA-CN-56/A-7-7.
- <sup>9</sup>J. L. Luxon and L. G. Davies, *Fusion Technol.* **8**, 441 (1985).
- <sup>10</sup>W. Howl, A. Turnbull, T. S. Taylor, L. L. Lao, F. J. Helton, J. R. Ferron, and E. J. Strait, *Phys. Fluids B* **4**, 1724 (1992).
- <sup>11</sup>E. J. Strait, L. Lao, A. G. Kellman, T. H. Osborne, R. Snider, R. D. Stambaugh, and T. S. Taylor, *Phys. Rev. Lett.* **62**, 1282 (1989).
- <sup>12</sup>R. Goldston, D. C. McCune, H. H. Towner, S. L. Davis, R. J. Hawryluk, and G. L. Schmidt, *J. Comput. Phys.* **43**, 61 (1981).
- <sup>13</sup>F. Levinton, R. J. Fonck, G. M. Gammel, R. Kaita, H. Kugel, E. T. Powell, and D. W. Roberts, *Phys. Rev. Lett.* **63**, 2060 (1989).
- <sup>14</sup>F. Troyon, R. Gruber, H. Saurenmann, S. Semenzato, and S. Succi, *Plasma Phys. Controlled Fusion* **26**, 209 (1984).
- <sup>15</sup>R. Bickerton, J. Connor, and J. B. Taylor, *Nature Phys. Sci.* **229**, 110 (1971).
- <sup>16</sup>J. Wesson and A. Sykes, *Nucl. Fusion* **25**, 85 (1985).
- <sup>17</sup>C. E. Bush, R. J. Goldston, S. D. Scott, E. D. Fredrickson, K. McGuire, J. Schivell, G. Taylor, Cris W. Barnes, M. G. Bell, R. L. Boivin, N. Bretz, R. V. Budny, A. Cavallo, P. C. Efthimion, B. Grek, R. Hawryluk, K. Hill, R. A. Hulse, A. Janos, D. W. Johnson, S. Kilpatrick, D. M. Manos, D. K. Mansfield, D. M. Meade, H. Park, A. T. Ramsey, B. Stratton, E. J. Synakowski, H. H. Towner, R. M. Wieland, M. C. Zarnstorff, and S. Zweben, *Phys. Rev. Lett.* **65**, 424 (1990).
- <sup>18</sup>M. Zarnstorff, M. G. Bell, M. Bitter, R. J. Goldston, B. Grek, R. J. Hawryluk, K. Hill, D. Johnson, D. McCune, H. Park, A. Ramsey, G. Taylor, and R. Wieland, *Phys. Rev. Lett.* **60**, 1306 (1988).
- <sup>19</sup>R. C. Grimm, M. S. Chance, A. M. M. Todd, J. Manickam, M. Okabayashi, W. M. Tang, R. L. Dewar, H. Fishman, S. L. Mendelsohn, D. A. Monticello, M. W. Phillips, and M. Reusch, *Nucl. Fusion* **25**, 805 (1985).
- <sup>20</sup>J. J. Ramos, *Phys. Rev. A* **42**, 1021 (1990).
- <sup>21</sup>R. L. Dewar, J. Manickam, R. C. Grimm, and M. S. Chance, *Nucl. Fusion* **21**, 493 (1981).
- <sup>22</sup>D. Lortz and J. Nuhrenberg, *J. Phys. Lett. A* **68**, 49 (1978).
- <sup>23</sup>L. Lao, T. Taylor, M. S. Chu, V. S. Chan, J. Ferron, and E. Strait, *Phys. Fluids B* **4**, 232 (1991).
- <sup>24</sup>M. C. Zarnstorff, C. W. Barnes, P. C. Efthimion, G. W. Hammett, W. Horton, R. A. Hulse, D. K. Mansfield, E. S. Marmor, K. M. McGuire, G. Rewoldt, B. C. Stratton, E. J. Synakowski, W. M. Tang, J. L. Terry, X. Q. Xu, M. G. Bell, M. Bitter, N. L. Bretz, R. Budny, C. E. Bush, P. H. Diamond, M. S. Chance, R. J. Fonck, E. D. Fredrickson, H. P. Furth, R. J. Goldston, B. Grek, R. J. Hawryluk, K. W. Hill, H. Hsuan, D. W. Johnson, D. C. McCune, D. M. Meade, D. Mueller, D. K. Owens, H. K. Park, A. T. Ramsey, M. N. Rosenbluth, J. Schivell, G. L. Schmidt, S. D. Scott, G. Taylor, and R. M. Wieland, in Ref. 1, p. 109.
- <sup>25</sup>J. Ferron, L. L. Lao, T. S. Taylor, Y. B. Kim, E. J. Strait, and D. Wroblewski, *Phys. Fluids B* **5**, 2532 (1993).
- <sup>26</sup>D. R. Mikkelsen, *Phys. Fluids B* **1**, 333 (1989).